

ARTICLES

Thermal and vibrational investigation of crystal nucleation and growth from a physically confined and supercooled liquid

R. Mu, Y. Xue, and D. O. Henderson*

Chemical Physics Laboratory, Department of Physics, Fisk University, Nashville, Tennessee 37208

D. O. Frazier

Space Science Laboratory, NASA Marshall Space Flight Center, Huntsville, Alabama 35812

(Received 21 April 1995; revised manuscript received 4 August 1995)

Differential scanning calorimetry and temperature-dependent Raman-scattering investigation of 2,4,6 trinitrotoluene (TNT) confined in four different pore-sized silica hosts have been conducted. The results suggested that (i) nucleation occurs at the pore center rather than at the pore walls; (ii) although the freezing transition of the bulk has a volume reduction of about 10%, the freezing transition of the confined phase maintains its interconnectivity; (iii) that TNT confined in 10-nm pores without bulk on the outer surface shows no freezing transition upon cooling and shows recrystallization and melting transitions upon heating suggests that the characteristic curves of nucleation and growth are modified resulting from the surface and physical confinement effects. In addition, our Raman study suggests that (i) the freezable confined TNT retains the similar solid structure to its bulk; (ii) the TNT physically confined in $d_p \leq 5$ -nm pores may exist in a cluster form.

INTRODUCTION

The study of the dynamic and thermodynamic properties of confined phases in various dielectric hosts is one of the important issues in nanometer scale technology. Well characterized porous media have been used as hosts: (1) to understand the physical confinement and the surface effects of the hosts on melting, freezing, and solid-solid transitions of the restricted phases inside pores,¹⁻⁹ (2) to illustrate the cluster formation and the possible mechanisms of crystal nucleation and growth in the condensed phase as well as in aqueous solution,⁸ (3) and to investigate molecular relaxation and diffusion in a restricted geometry.⁹

It is known that when fluids and solids are restricted in nano-sized pores, their freezing and melting transition temperature will be depressed.¹⁻⁹ However, how and where the nucleation occurs is still not clear and sometimes controversial. In addition, how the physical confinement and surface properties modify the confined phase structure has not been well-established. The plug model proposed by Awschalom and co-workers¹ predicts that the depression of freezing, melting, and solid-solid transition temperatures of the confined phases are inversely proportional to the average pore size and are consistent with experimental data. A molecular-dynamics (MD) simulation study⁶ of molecular freezing dynamics of a Lennard-Jones liquid in a confined geometry has predicted the time development of ordering and a freezing mechanism. Upon cooling, the confined liquid forms layers near the pore wall and a subsequent in-plane ordering within a layer which is accomplished by a sharpening of the layering in the transverse direction, which has been qualitatively supported by neutron-scattering experiments of Sokol *et al.*⁴ However, the MD simulation⁴ cannot provide information on

supercooling effects for confined fluids. The correlation between the supercooling effect and the structure of the confined phase is lacking. In addition, the mechanism of the nucleation and growth from the supercooled and confined fluids in porous media is not yet well understood.

The motivation of the present research is to use 2,4,6-trinitrotoluene (TNT) as a prototype of molecular systems which exhibits large undercooling (i) to illustrate how and where the solid nucleation occurs in porous media when the fluid is supercooled, (ii) to demonstrate how bulk TNT outside the pores alters the freezing properties of the confined phase, (iii) to examine how the structure of the confined TNT and its percolation behavior are modified before and after the freezing and melting transitions.

In the past several years, TNT has been extensively studied in our laboratory. Its thermal, optical, and TNT-metal oxide interaction properties are relatively well known. Bulk TNT exhibits a supercooling effect of more than 35 K, which makes TNT a good candidate for investigating supercooling phenomena in the confined state. In addition, an understanding of TNT cluster formation and cluster thermodynamics is very important for the design of explosive detection devices.

EXPERIMENTAL

2,4,6-TNT was purchased from Chem Service with purity of 99.0%⁺. As-received TNT contains 10–20% water. In order to remove the added water and to further purify the sample, the TNT was transferred into a cleaned quartz tube which connected to a mild vacuum. The tube with the sample was placed into a furnace with temperature gradient from 393 to 300 K with the span of 9 in. The sample was placed at the hottest spot. First, the adsorbed water can be pumped out

via vacuum pump. Then, the other impurities and TNT, depending upon their vapor pressure and their boiling points, were condensed onto the inside wall of the quartz tube in different zones. Then the tube was cut into different sections. With thermal differential scanning calorimetry (DSC) and optical (IR) analysis, the purest polycrystalline TNT was identified and used in the subsequent measurements.

Gelsil porous silica discs with pore diameters of 20, 10, 5, and 2.5 nm were used for confining the TNT. To clean the Gelsils, the glass was first moisturized in the humidity controlled chamber over 24 h before being immersed into pure water. The discs were cut into suitable sizes for further use in the experiments. The cut pieces were immersed into 30% H_2O_2 solution and heated up to 373 K for 12 h to remove organic contamination in the glass. The glasses were then rinsed many times with 18 M Ω ultrapure water. The cleaned Gelsil substrates were stored in the large volume of ultrapure water until further use.

The impregnation of TNT into Gelsils involves two steps. In the first step, the cleaned glass was transferred into a quartz tube and dried under vacuum at the pressure of 10^{-5} torr at the temperature of 723 K for 6 h. Then the temperature was reduced to 298 K and the sample tube was back-filled with ultrapure nitrogen gas. A sufficient amount of the purified TNT was loaded into the tube. The vacuum pump was slowly turned back on. After the 2–3 h pumping, the quartz tube was isolated from the vacuum and the sample was melted at 363 K and maintained at that temperature for 1 h to allow liquid TNT to flow into the silica pores. Then, the impregnated Gelsil glasses were slowly cooled back to room temperature.

The thermal measurements were performed with a Perkin-Elmer differential scanning calorimeter (DSC 2) and a TA modulated DSC 2920 in the range of 100–380 K. In order to optimize the quality of the measurements, four different heating and cooling rates of 10, 5, 2, and 1 K/min were used. No dramatic temperature drifting was observed for different ramping rates. To enhance the signal-to-noise ratio, 5 K/min heating and cooling rates were used throughout the measurements.

Temperature-dependent Raman-scattering measurements of TNT in its bulk and confined phases were carried out with a Spex Raman spectrometer equipped with a double-grating monochromator and an Ar^+ laser. The scattered light was collected at 90° to the incident laser beam. A homebuilt variable temperature cell was used to control the temperature with a stability $< \pm 2$ K. A typical 1-cm^{-1} resolution and 2 s integration time were used throughout the measurements. Spectra were collected between 10 and 230 cm^{-1} from the excitation line ($19\,436\text{ cm}^{-1}$) at a power of 100 mW.

RESULTS AND DISCUSSION

A. Thermal properties of the confined TNT

Figures 1 and 2 show the DSC thermograms of the confined TNT with and without bulk TNT on the outer surface for pore diameters of 10 and 20 nm. For the TNT confined in 2.5- and 5-nm pores only the bulk TNT melting and freezing transitions were observed indicating that the TNT physically restricted in 5-nm pores is incapable of freezing. For the TNT confined in 10-nm pores, as shown in Fig. 1, two dif-

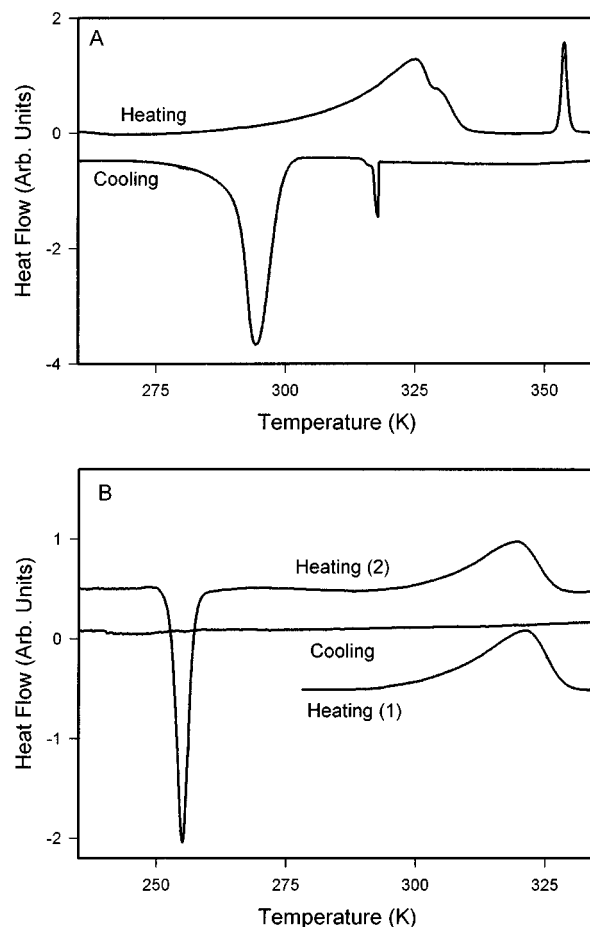


FIG. 1. DSC thermograms of TNT physically confined in 10-nm pores. (A) with excess bulk TNT on the outer surface of the porous silica; (B) no presence of bulk TNT.

ferent freezing processes were observed. The confined TNT with the bulk at the outer surface in Fig. 1(A) exhibited two melting and two freezing peaks upon the heating and cooling runs. The two broad phase transitions at lower temperature $T_{mc}=323$ K and $T_{fc}=288$ K are due to the melting and freezing transitions of the confined TNT, while the two sharp peaks at $T_{mb}=353$ K and $T_{fb}=319$ K are due to the melting and freezing transition of the bulk TNT on the outer surface. When the bulk TNT was removed, as is shown in Fig. 1(B), the melting curve of the confined TNT mimics the melting behavior of the confined TNT in Fig. 1(A). However, upon cooling, no freezing transition was observed. In a subsequent heating run, an exothermic transition occurs at ~ 250 K before the observation of the melting transition of the confined TNT at 321 K. For TNT confined in 20-nm pores with excess bulk covering the silica surface, as depicted in Fig. 2(A), two melting peaks were observed. Clearly, the broad peak at $T_{cm}=340$ K is the melting transition of the confined TNT and the sharp one at $T_{bm}=352$ K is the melting transition of bulk TNT. Interestingly, when the sample was cooled, only one strong and sharp transition at $T_{(b+c)f}=319$ K was observed suggesting that both the bulk and the confined TNT freeze at the same temperature. Figure 2(B) further shows that the confined TNT without the presence of the bulk exhibits a similar broad melting transition at $T_{cm}=340$ K and a sharp freezing transition at $T_{cf}=287$ K rather than at 319 K.

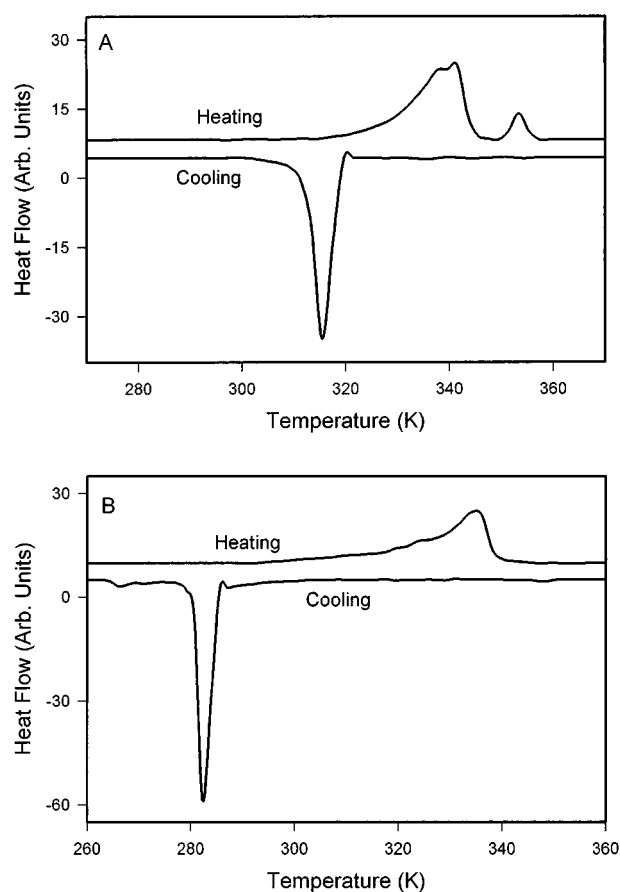


FIG. 2. DSC thermograms of TNT physically confined in 20-nm pores. (A) with excess bulk TNT on the outer surface of the porous substrate; (B) no bulk TNT presence.

1. TNT physically confined in 5-nm pores

As demonstrated by us⁸ and others,^{3,7} when a fluid or a solid is restricted in ultrasmall pores, a bulk-to-clusters crossover effect can be observed. For TNT physically restricted in 5-nm silica pores, with and without bulk TNT covering the outer surface, only the bulk TNT melting and freezing transition resulted and no freezing and melting transitions of the confined TNT were observed indicating that the TNT in such small pores is incapable of freezing. This observation may be attributed to two reasons: (1) freezing of the confined TNT in pores requires a relatively larger critical nucleus size with respect to smaller organic molecules, such as cyclohexane,^{2,3,7} (2) TNT can be strongly adsorbed on the silica surface through hydrogen bonding. The adsorbed TNT molecules are immobilized and not able to participate in the nucleation process. This, in turn, reduces the number of molecules available to form a critical nucleus. Based on the orthorhombic cell parameters¹⁰ ($a=14.991$ Å, $b=6.077$ Å, and $c=20.017$ Å) of a TNT single crystal, only 2–8 unit cells can exist across the 5-nm pores. Therefore, the TNT confined in such small pores may be in the cluster form rather than in a conventional solid or liquid phase. As we will discuss later, our Raman spectroscopic investigation further supports this point.

2. TNT physically confined in 10- and 20-nm pores with bulk on outer surface

The characteristics of the melting transitions of confined TNT in 10- and 20-nm pores are very similar to the observations in other systems.^{1–3} There are two melting transitions observed in both systems. The broad and lower temperature transition is due to the melting transition of the confined phase. The smaller the pore sizes are, the lower the melting transition temperature becomes. The broadness of the transition can be attributed to two causes. One is due to the finite-size effect. It is known that first-order phase transitions are infinitely sharp only at the thermodynamic limit. ($N \rightarrow \infty$ at constant density, and N is the number of molecules in the system.) For a finite number of molecules N , the phase transition acquires a finite width at the transition temperature. Sheng, Cohen, and Schrieffer¹¹ and Imry¹² have studied melting transition of small molecular clusters and a finite-size rounding effect of a first-order phase transitions. The specific heat of small clusters exhibits a broadened peak centered at the temperatures below the bulk transition temperature. As the cluster size decreases, the peak tends to broaden. The finite-size broadening is estimated to be proportional to the inverse of the product of the system size N and the latent entropy of the transition.¹² The other is due to the finite pore-size distribution of each substrate used since the phase transition temperature of confined TNT is inversely proportional to the pore size. However, when the systems are cooled, the TNT in 10- and 20-nm pores exhibits very different freezing behavior. For the TNT confined in 10-nm pores, two freezing transitions were also observed. The sharp freezing transition at the higher temperature is due to freezing of the bulk phase, while the lower temperature transition is due to freezing of confined TNT. For the TNT confined in 20-nm pores, only *one* freezing transition is observed. The total amount of the energy released during the freezing process is equal to the total intake energy of the bulk and the confined TNT during the melting transitions. This suggests that the bulk and the confined TNT freeze at the same time. The freezing process starts at the outer surface and penetrates into the porous glass through the interconnected pores. Due to the potentially strong hydrogen bonding between the adsorbed TNT and silica surface, the propagation process is expected to occur through the pore center. Therefore, our experimental results support the Scherer's theoretical argument that when the porous media is immersed in a pool of fluid that is undercooled, the crystallized solid phase outside the porous media can act as a seed for the confined fluid to freeze.^{5,13} The degree of the solid "invasion" into the pores is dictated by the growth thermodynamics, i.e., the total Gibbs free energy change (ΔG_{total}) must be less than or equal to zero. Therefore, it is suggested that the solid invasion will be stopped at the throat¹³ (the smallest pore size of the media). On the other hand, a computer simulation by Ma, Banavar, and Koplik⁶ suggests that the fluids inside the pores freeze layer by layer initiating from the wall, then, one would expect the small pores would freeze first. The bulk on outer surface has little to do with the confined TNT inside pores. However, the results for the TNT confined in 20-nm pores with bulk on the outer surface strongly suggest that the freezing of the bulk

TNT can indeed trigger the freezing transition of the confined TNT inside the pores. At the bulk freezing temperature T_{bf} , all the confined TNT molecules are also in the supercooled state, i.e., $T_{bf} < T_{cm}$. For the TNT in 10-nm pores, the freezing transition of the bulk TNT can only trigger a fraction of the confined TNT in larger pores of the substrate to freeze. However, the freezing process is terminated at the throats or smaller pores interconnecting the larger pore of the disk since the TNT in small pores is still thermodynamically favored to be in the liquid phase. Therefore, the freezing process is annihilated by these small pores—throats. If the interconnectivity of the large pores is below their percolation threshold, then the large pores inside the porous glass will remain in supercooled liquid phase. As a result, with the presence of the bulk, the confined TNT in 10-nm pores gives its own freezing transition temperature at 288 K. Therefore, the present results suggest that (1) the solid phase can indeed act as a seed to trigger a heterogeneous nucleation of the confined TNT by penetrating into the porous media, (2) during the freezing process, the TNT still reserves the interconnectivity. However, it is known that when the TNT freezes from its liquid state, a 10% volume reduction is expected. The interconnectivity of the confined TNT seems to suggest that the volume shrinkage is considerably reduced.

3. TNT confined in 10- and 20-nm pores without bulk TNT on the surface

As discussed in the previous paragraph, the TNT confined in 20-nm pores should render a sharp freezing transition at much lower temperature which is consistent with our experimental observation shown in Fig. 2(B). The sharp transition is due to the crystallization of the TNT in large pores which triggers all the confined TNT to freeze since all the confined TNT is supercooled $T_{cf} < T_{cm}$. However, when the TNT is confined in 10-nm pores, an additional feature is illustrated. That is, when the bulk TNT was removed from the outer surface of the impregnated porous glass ($d_p = 10$ nm), an endothermic peak at 250 K and an exothermic peak at 323 K were observed upon the second heating. When the system is cooled, no freezing transition was observed up to 100 K. This observation seems to be independent of cooling rate (> 1 K/min). Since the second peak at $T_{cm} = 323$ K coincides with the melting transition of the confined TNT during the very first heating, it, therefore, can be argued that the peak at $T = 323$ K is due to the solid melting transition of the confined TNT, while the exothermic peak at $T_x = 250$ K is believed to be due to the crystallization. There are two explanations that may account for the present observation. In the context of classic nucleation and growth theories,¹⁴ for an undercooled liquid to freeze, a nucleus must first be formed. This is followed by a growth process. It is also known that the nucleation rate and growth rate do not follow the same temperature-dependent characteristics. A freezing transition can only exist when the nucleation and growth curves overlap, which is apparently the case for bulk TNT and the confined TNT in 20-nm pores. However, as the physical dimension of the confined TNT is reduced, the confined TNT will experience two effects: one is the surface adsorption and perturbation from the substrate and the other is the modification of the thermodynamic properties from its bulk due to the finite-size effects. The surface adsorption process will

immobilize the TNT molecules near or close to the substrate surface which (i) reduces the nucleus formation frequency and (ii) decreases the crystal-growth process by reducing molecular diffusion. The finite-size effect will modify the intermolecular interaction and increase the disorderness.¹² Therefore, it may be expected that these two effects will result in different shifts between the temperature-dependent nucleation and growth curves, which will in turn result in further separation of these two curves. Namely, the nucleation curve shifts to a lower temperature region whereas the growth curve shifts to a higher-temperature region. In fact, earlier studies⁹ have suggested that the dynamic process of the confined fluids is decreased and the structure of the confined liquids can be highly perturbed especially when the fluid wets the substrate surface. As a result, the nucleation and growth curves may have little overlap in the temperature domain. Upon cooling, when the growth rate is nonzero at higher temperature, the nucleation rate is virtually zero. While the nucleation rate is nonzero at rather low temperature, the growth rate is quenched. Therefore, no freezing transition is possible. However, during the cooling process, nuclei have been formed at lower temperature. When the system is heated up to the temperature at which the growth rate is nonzero, the formed nuclei will lead to a crystallization transformation. The other explanation is that the interfacial energy at fluid/wall interface may show hysteresis effect depending on cooling or heating at low temperature $T < 250$ K. That is, when the system is cooled to the crystallization temperature at $T_{cc} = 250$ K, the interfacial energy σ is large. The confined TNT still remains in the liquid state. The further cooling will result in the vitrification of the fluid TNT in pores. The differential thermal properties of the rigid vitrified TNT and silica substrate, such as thermal expansion, may cause the physical separation between the confined TNT and the substrate. In fact, 10% volume shrinkage has been found when TNT transforms from the liquid phase to solid phase. As a result, the interfacial energy may be reduced. Upon heating, the reduced interfacial energy decreases the crystallization barrier which leads to the observation of crystallization at $T_{cc} = 250$ K.

B. Temperature-dependent Raman measurements

1. Raman scattering of bulk TNT at 10–230 cm^{-1} (290–355 K)

In order to identify the structure of confined TNT in pores of various sizes and at different temperatures, temperature-dependent Raman scattering of polycrystalline bulk TNT was first investigated. Figure 3 shows a representative set of Raman spectra at different temperatures upon the heating and cooling runs. Five peaks at 23, 56, 108, 159, and 190 cm^{-1} are observed in the 10–230 cm^{-1} region. The bands below 160 cm^{-1} disappeared when the TNT was in the liquid state, and the band at 190 cm^{-1} experienced an abrupt frequency shifting and linewidth broadening. Although there has been no detailed vibrational analysis on TNT, the bands below 160 cm^{-1} may be attributed to lattice modes. The study¹⁵ of low-frequency Raman and infrared spectra of an *m*-chloronitrobenzene single crystal suggests that the band at ~ 93 cm^{-1} is the NO_2 torsion. Stewart, Bosco, and Carpenter¹⁶ have assigned the C-N-O bend vibration to be at 70 cm^{-1} . It also seems possible that the band at 108 cm^{-1}

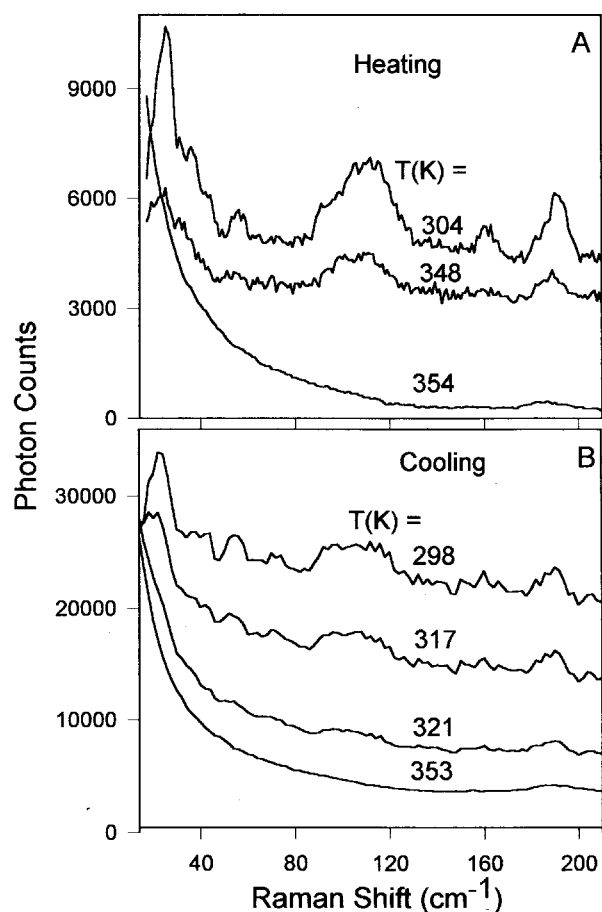


FIG. 3. Temperature-dependent Raman spectra of bulk TNT. (A) heating run; (B) cooling run.

may be due to the C-N-O bend. However, the disappearance of this band upon melting fails to support the case. Therefore, the band at 108 cm^{-1} is most likely to be the NO_2 torsion mode. The characteristics of the frequency and linewidth of the band at 190 cm^{-1} indicates that this mode may be assigned to librational modes of the NO_2 rather than a lattice mode due to two reasons: (1) lattice vibrations vanish when TNT melts, while the mode at 190 cm^{-1} only experienced a sudden change in linewidth and frequency, (2) the linewidth of the mode at 190 cm^{-1} is almost doubled when the TNT is in the liquid state indicating that the vibration is sensitive to its environment, i.e., intermolecular interaction. A molecular crystal structural investigation by Carper, Davis, and Extine¹⁰ suggests that the major intermolecular interactions in the TNT single crystals are hydrogen bonding. The hydrogen bonding is formed between the oxygen atom in one molecule and a hydrogen atom from an adjacent molecule. Once the system is in the liquid state, the intermolecular bonding is highly modified due to the onset of rotational and translational motion of each molecule. The intermolecular hydrogen bonding may be described as having bond forming and breaking characteristics. It seems that the temperature-dependent behavior of the band at 190 cm^{-1} can closely reflect the aforementioned characteristics. Therefore, the band at 190 cm^{-1} is attributed to the librational mode of NO_2 groups. The low-frequency mode at 23 cm^{-1} is assigned to a lattice phonon. Figure 4 shows the temperature-dependent

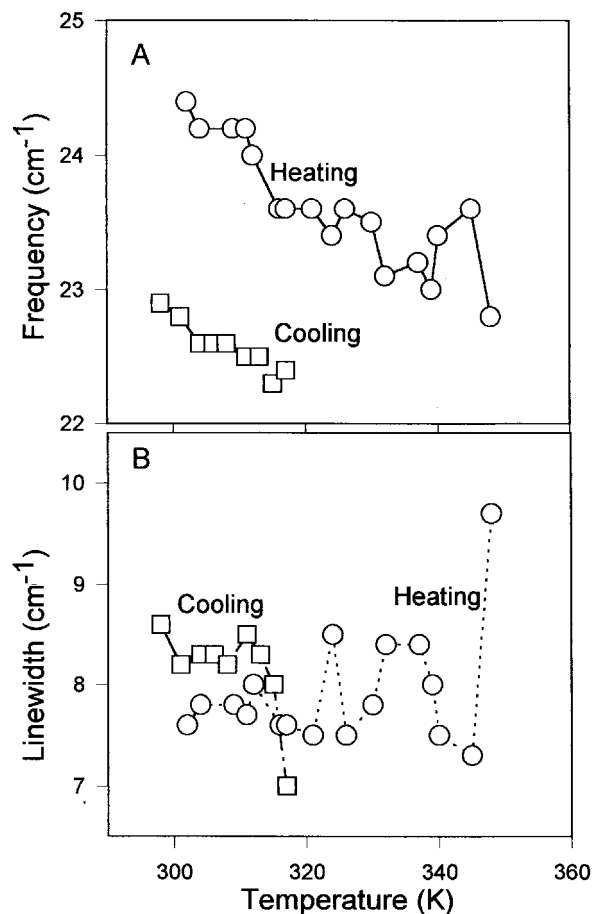


FIG. 4. Temperature-dependent characteristics of the bands at 23 and 190 cm^{-1} upon heating and cooling runs.

behavior of the bands at 190 and 23 cm^{-1} , respectively. The disappearance of the band at 23 cm^{-1} at 373 K during heating suggests the melting transition. The sudden reappearance at 317 K upon cooling indicates that the bulk TNT was supercooled as low as 317 K before freezing. The frequency shifting of the band at 190 cm^{-1} can also be related to the orderedness of the solid phase formed from supercooling. Further, it is anticipated that when the TNT is confined in ultrasmall pores, the band at 23 cm^{-1} can reflect the solid structure of the TNT, while the band at 190 cm^{-1} may provide information on TNT-substrate interactions.

2. Raman investigation of melting and freezing transitions of the confined TNT

As stated earlier, the confined TNT in each pore of various sizes has been subdivided into two sets. One is the sample with bulk TNT covering the outer surface. The other is the sample with no bulk TNT on the surface. The temperature-dependent Raman-scattering investigation shows that the freezing transition of the confined TNT has a strong correlation with the presence or absence of the bulk TNT on the sample surface as discussed in the previous section. The melting transition of the confined TNT without bulk TNT on the surface only shows the pore-size dependence. Table I summarizes the observed freezing and melting transition temperatures of the confined TNT in four

TABLE I. Melting and freezing transition temperatures of bulk and the confined TNT via Raman-scattering measurements.

Confined TNT in d_p (nm)=	Bulk TNT	20 nm w/bulk presence	20 nm w/o bulk presence	10 nm w/bulk presence	10 nm w/o bulk presence	5 nm w/ & w/o bulk	2.5 nm w/ & w/o bulk
Melting	352±2 K	340±2 K	338±2 K	323±2 K	320±2 K		
Freezing	318±2 K	319±2 K	287±2 K	288±2 K	? ^a		

^aThe confined TNT in 10 nm pores can crystallize upon heating from 100 K. The crystallization temperature is at ~251 K, based on DSC measurements.

different pore sizes together with the bulk TNT. The results obtained from temperature-dependent Raman measurements are consistent with DSC measurements.

3. Structural characterization of the confined TNT in different pore sizes

As discussed earlier, two vibrational modes at 23 and 190 cm^{-1} , respectively were chosen to investigate the confined TNT in different pore-sized silica hosts. These two modes not only give the information on the phase transition, but they may also provide structural characteristics of the TNT confined in the pores. Table II summarizes the observed band frequencies and their linewidths for bulk TNT and confined TNT.

Based upon the center frequencies and the linewidths of the bands at 23 and 190 cm^{-1} , it is clear that the solid phase of the confined TNT shows a very close resemblance to that of the bulk TNT. During the melting transition, the disappearance of the band at 23 cm^{-1} indicates the lattice phonon is destroyed. Like the bulk, the band at 190 cm^{-1} exhibits two trends. That is, the frequency of the band redshifts by ~2 cm^{-1} , while the linewidth is broadened by ~6–10 cm^{-1} . In addition, the band at 190 cm^{-1} for the confined TNT seems to be less sensitive to the temperature. When the system is heated up to 375 K, the band for the confined TNT at 190 cm^{-1} is redshifted by ~2 cm^{-1} , while the bulk frequency shifts by 6 cm^{-1} . It can be argued that the NO_2 groups of the confined TNT can form hydrogen-bonding with the OH groups on pore surfaces. Therefore, the NO_2 librational mode is further constrained by increasing the hindered rotational barrier height.

C. Mechanism of nucleation and growth of confined TNT in porous silica

Although the question has been addressed many times as to where and how nucleation and growth occur when a fluid is confined in porous media, the answer is often inconclusive and controversial. Fortunately, the present DSC and Raman investigation clearly shows that crystal nucleation and growth processes start at the center of the pores rather than from the pore wall via layer-by-layer formation. This statement can be supported by the following experimental results and arguments: (1) Freezing and melting transition temperatures of the bulk TNT are independent of the presence of the porous substrates suggesting that the silica surface does not cause heterogeneous nucleation; (2) the absence of the freezing and melting phase transition characteristics, when the TNT is confined in 5-nm pores with and without the presence of bulk TNT, suggests that TNT-silica interaction is stronger than intermolecular interaction of TNT. The adsorbed TNT molecules on the silica surface are unable to participate in the freezing transition since there are not enough TNT molecules at the pore centers to form a solid phase. However, in the case of the TNT physically confined in 10- and 20-nm pores, bulk TNT can trigger the freezing transition for confined TNT indicating that the crystal-growth process must proceed through the centers of the pores; (3) the fact that a much lower freezing transition temperature is observed for the confined TNT without the presence of the bulk than that of the sample with the bulk TNT confirms that the silica surface can not facilitate heterogeneous nucleation. In addition, the fact that for very small pores, $d \leq 5.0$ nm, no freezing transition is observed as low as 100 K which also sug-

TABLE II. The observed frequencies and the linewidths of the bands at 23 and 190 cm^{-1} for the bulk and the confined TNT at selected temperatures. The data provided in the table are in cm^{-1} . The data outside the parentheses are the observed center frequency, while the data inside the parentheses are the linewidths of the band.

Confined TNT in d_p (nm)=	Bulk TNT	20 nm w/ bulk	20 nm w/o bulk	10 nm w/ bulk	10 nm w/o bulk	5 nm w/ & w/o bulk	2.5 nm w/ & w/o bulk
Before melting	24 (8)	23 (6)	24 (5)	23 (5)	24 (5)		
After melting	192(12)	190(12)	191(12)	190(13)	191 (14)	191(20) ^a	189(20)
After freezing	186(23)	188(23)	189(20)	188(19)	188 (20)	191 (20)	?
Before melting	23 (8)	23 (6)	24 (5)	23 (4)			
After melting	190(11)	190(12)	191(12)	191(13)	190(20) ^a	190(19) ^a	?

^aIndicates that the sample shows no melting or freezing transition.

gests that the TNT-silica surface interaction is long range. The perturbation from the substrate surface prohibits the possible crystallization of the confined TNT. Therefore, the only possible conclusion is that nucleation must occur at the pore center; (4) Raman measurements further show that the solid TNT formed in the pores has the conventional orthorhombic structure as the bulk TNT does. Therefore, we must conclude that the silica surface can not cause heterogeneous nucleation and the nucleation occurs at the pore center.

CONCLUSION

The thermodynamic investigations of the TNT confined in 5-, 10-, and 20-nm pores suggests that nucleation occurs at the pore center rather than at the pore wall surface; (i) although the freezing transition of the bulk has a volume reduction of about 10%, the freezing transition of the confined phase maintains its interconnectivity; (ii) that TNT confined in 10-nm pores without bulk on outer surface shows no

freezing transition upon cooling and shows recrystallization and melting transitions upon heating suggest that the characteristic curves of nucleation and growth are modified resulting from the surface and physical confinement effects. Temperature-dependent Raman-scattering measurements of bulk and confined TNT in pores of four different sizes further support the DSC results. In addition, the results also suggest that (i) the freezable confined TNT retains the similar solid structure to its bulk; (ii) the TNT physically confined in 5- and 2.5-nm pores may exist in a cluster form.

ACKNOWLEDGMENTS

This work was supported by NASA under Grant No. NAG8-1066 and also from the Federal Aviation Administration (FAA) Under Grant No. 93-G-057. In addition, acknowledgment also goes to TA Instrument for using their DSC 2920 and their technical assistance.

* Author to whom correspondence should be addressed.

¹D. D. Awschalom and J. Warnock, *Phys. Rev. B* **35**, 6779 (1987); J. Warnock, D. D. Awschalom, and M. W. Shafer, *Phys. Rev. Lett.* **57**, 1753 (1986).

²R. Mu and V. M. Malhotra, *Phys. Rev. B* **44**, 4296 (1991).

³C. L. Jackson and G. B. McKenna, *J. Chem. Phys.* **93**, 9002 (1990).

⁴P. E. Sokol, W. J. Ma, K. W. Herwig, W. M. Snow, Y. Wang, J. Koplik, and J. R. Banavar, *Appl. Phys. Lett.* **61**, 777 (1992).

⁵George W. Scherer, *J. Non-Cryst. Solids* **155**, 1 (1993).

⁶W. J. Ma, J. R. Banavar, and J. Koplik, *J. Chem. Phys.* **97**, 485 (1992).

⁷A. Brodka and T. W. Zerda, *J. Chem. Phys.* **97**, 5676 (1992).

⁸R. Mu, F. Jin, S. H. Morgan, D. O. Henderson, and E. Silberman, *J. Chem. Phys.* **100**, 7749 (1994); R. Mu, D. O. Henderson, and F. Jin, in *Determining Nanoscale Physical Properties of Materials by Microscopy and Spectroscopy*, edited by M. Sarikaya, M. Isaacson, and H. K. Wickramasinghe, MRS Symposia Proceed-

ings No. 332 (Materials Research Society, Pittsburgh, 1994), pp. 243–248.

⁹J. Klafter and J. M. Drake, *Molecular Dynamics in Restricted Geometries* (Wiley, New York, 1989).

¹⁰W. R. Carper, L. P. Davis, and M. W. Extine, *J. Phys. Chem.* **86**, 459 (1982).

¹¹P. Sheng, R. W. Cohen, and J. R. Schrieffer, *J. Phys. C* **14**, L565 (1981).

¹²Y. Imry, *Phys. Rev. B* **21**, 2042 (1980).

¹³R. Mu, Ph.D. thesis, Southern Illinois University, 1992.

¹⁴J. Zarzycki, *Glasses and the Vitreous State*, Cambridge Solid State Sciences Series (Cambridge University Press, Cambridge, 1991).

¹⁵N. LeCalve, F. Romain, and B. Pasquier, *J. Raman Spectrosc.* **8**, 239 (1979).

¹⁶J. J. P. Stewart, S. R. Bosco, and W. R. Carper, *Spectrochim. Acta* **42A**, 13 (1986).